



Stochastic Optimization-Based hosting capacity estimation with volatile net load deviation in distribution grids

Yongjun Cho, Eunjung Lee, Keon Baek, Jinho Kim^{*}

Gwangju Institute of Science and Technology, School of Integrated Technology, Gwangju 61005, Republic of Korea

HIGHLIGHTS

- The proposed framework contributes to alleviating the net load variability problem caused by the over-penetrated VRE capacity.
- The framework effectively captured the net load deviation intensity and magnitude without losing consistency in conservative results.
- To consider the volatilities and uncertainties of VRE and loads, a multi-time stochastic optimization model was formulated.
- To evaluate the economic effect, the estimation of the accommodation costs for VREs was compared with the results of the conventional HC model.

ARTICLE INFO

Keywords:

Distribution grid
Hosting capacity
Mixed-integer linear programming
Net-load deviation
Stochastic optimization

ABSTRACT

With the increasing penetration rates of variable renewable energies (VREs), estimating the maximum network capacity without adversely impacting the reliability or voltage quality for power system operation, that is, the hosting capacity (HC), is a significant issue. For system operators, it is challenging to secure flexible resources that can respond to the volatility of the net load resulting from the intermittent generation characteristics of VREs and the appearance of various consumers. Thus, this study proposed a hosting capacity estimation framework that considers the net load deviation. It thereby overcomes the abrupt net load deviation for the economic accommodation of VREs. To evaluate proposed framework, the qualification of the proposed net load deviation limit as a new performance index and investigation for improving HC was verified via performance violation analysis. The proposed net load filter exhibited excellent performance in capturing the net load deviation without distorting the conventional performance index. To consider the net load deviation magnitude and intensity effect on system operation, a multi-time stochastic optimization model was formulated. The proposed framework was tested on an IEEE 33-radial bus system to investigate the effects of the net load deviation limit on the HC, and its potential as a performance index was analyzed. Finally, as an application of the proposed model to help the system operator's precise decision making, the VRE accommodation costs was quantitatively suggested.

1. Introduction

1.1. Research background & motivation

The increase in greenhouse gas emissions has resulted in a climate change crisis that has resulted in the declaration of the Climate Ambition Alliance (Net Zero 2050) being signed by 121 countries. According to this declaration, each country should set and implement a nationally determined contribution to achieve net-zero emissions by 2050. To achieve net-zero emissions by 2050, 1,020 GW of photovoltaic (PV) power and wind turbine (WT) power capacity per year should be

installed by 2030 [1]. These variable renewable energies (VREs) are distributed and small in capacity, and their dispatchability cannot be guaranteed. This paradigm shift in power generation resources results in challenging issues for both transmission and distribution network operations. At the level of distribution system, the prevailing “fit-and-forget” approach, where a “firm connection guarantees that the installed capacity does not exceed capacity limits set by the distribution system operators (DSOs), has introduced technical operation problems of distribution system, such as over-voltages, increased losses, thermal overloading, and reverse flow problems [2–4]. At the transmission level, abrupt net load deviation due to intermittent characteristics of VREs results in balancing issues that necessitate securing the system's

^{*} Corresponding author.

E-mail address: jeikim@gist.ac.kr (J. Kim).

<https://doi.org/10.1016/j.apenergy.2023.121075>

Received 9 December 2022; Received in revised form 22 March 2023; Accepted 1 April 2023

Available online 19 April 2023

0306-2619/© 2023 The Authors. Published by Elsevier Ltd. This is an open access article under the CC BY-NC license (<http://creativecommons.org/licenses/by-nc/4.0/>).

Nomenclature			
Sets			
C_i	Set of points of interconnection connected to bus i	PL_{ij}^{max}	Maximum active power flow of line ij
T	Set of time periods	QL_{ij}^{max}	Maximum reactive power flow of line ij
B	Set of buses	$P_{c,t}^{M,max}$	Maximum active power exchanged between the upstream grid and distribution network at point c , over time t
L	Set of lines	$\Delta P_c^{M,max}$	Maximum net load deviation intensity of power exchanged between the upstream grid
L_i	Set of lines connected to bus i		
Indices		Variables	
c	Index for points of interconnection	C_i^{PV}	Number of installed unit PV at bus i
i,j	Index for buses	C_i^{WT}	Number of installed unit WT at bus i
t	Time period	$P_{i,t}^D$	Active power load at bus I at time t
Parameters		$Q_{i,t}^D$	Reactive power load at bus I at time t
$P_t^{PV,gen}$	Unit PV active power generation, over time t	$P_{c,t}^M$	Active power exchange with upstream grid at point of interconnection c at time t
$P_t^{WT,gen}$	Unit WT active power generation, over time t	$Q_{c,t}^M$	Active power exchange with upstream grid at point of interconnection c at time t
$Q_t^{PV,gen}$	Unit PV reactive power generation, over time t	$PL_{ij,t}$	Active power flow at line ij at time t
$Q_t^{WT,gen}$	Unit WT reactive power generation, over time t	$QL_{ij,t}$	Reactive power flow at line ij at time t
b_{mn}	Susceptance of line ij	$V_{i,t}$	Voltage magnitude of bus i at time t
g_{mn}	Conductance of line ij	$\theta_{i,t}$	Voltage angle in bus i at time t
r_{ij}	Resistance of line ij	$\Delta V_{i,t}$	Voltage magnitude deviation of bus i at time t
x_{ij}	Reactance of line ij	$\Delta \theta_{i,t}$	Voltage angle deviation in bus i at time t
ΔV_i^{max}	Upper limit of voltage magnitude deviation at bus i		
ΔV_i^{min}	Lower limit of voltage magnitude deviation at bus i		

flexibility. Because conventional bulk power generators have a ramp-up/down limit, they may be unable to handle sudden fluctuations. Whereas, for power systems with high VRE penetration rates, only a few hours of abrupt net load variation have a decisive effect on the power system [5].

The distribution network, which is a direct connection point of VREs, is threatened with stable operation by the intermittent characteristics of VREs. To manage this risk, DSOs may consider various strategies utilizing additional resources such as ESS and flexible resources. Although such active network management has been actively researched, practical implementation of hindered owing to the uncertainty regarding the topology of the system [6]. Therefore, the DSO should preferentially estimate the possible capacity for VREs in a distribution network without adversely impacting the reliability or voltage quality for system operation, that is, hosting capacity (HC). In future power systems, market design will be advanced to expand to network-related services as well as energy-related services to maximize the potential of distributed resources [7]. To successfully transition towards the trend of this era, the DSO requires an unbiased and analytical evaluation of HC to efficiently manage and operate distributed resources within the system. This can be achieved with sophisticated HC estimation framework.

At the transmission system level, owing to the thrives of VREs, Transmission System Operators(TSO) are experiencing considerable difficulties in the most important supply–demand balance responsibility. To solve this, TSOs are making various efforts and attempts. For example, lowering the market’s clearing resolution to reduce forecasting errors, increasing reserve margins, or introducing new markets such as flexible ramping products (FRPs) [8]. FRP has been recently launched in electricity markets to enhance the power grid flexibility and accommodate netload deviation’s uncertainty introduced by renewable energy resources. However, these measures also require TSO to secure the flexibility by procuring flexible resources that would otherwise have been involved in other markets at an additional cost as well.

As confirmed above, DSO and TSO are making their own efforts to achieve the green energy transition. As the proportion of VREs in the distribution system increases, the distribution system will evolve into an active distribution network with dispatchability rather than a passive

source of demand [9]. However, owing to the VRE’s low installed capacity and uncertainties, the net load variability at the interconnection point between transmission and distribution will become more serious, and eventually, it will have a great detrimental effect on maintaining the real-time supply–demand balance on transmission level. Consequently, customers will bear all the burden caused by the indiscriminate integration of renewable energy.

1.2. Literature reviews

This chapter introduces the latest research trends on hosting capacity estimation framework. In particular, the performance indices and simulation method, which are the core of the framework, are described.

1.2.1. Hosting capacity’s performance index reviews

To estimate HC, we must first consider the performance index. This makes the concept of HC practical by employing system parameters as an assessment criterion for VRE penetration [5]. The performance indices may include voltage, frequency fluctuation, transformer thermal limit, power quality, and protection required for reliable power system operation. In addition, the acceptable variation of radial distribution feeder performance is identified by voltage limits, thermal capacity, and imbalance [11]. Overvoltage and thermal overloading indices are primarily considered because they are key components in distribution system operation. A previous study investigated the impact of surplus power on feeders and found that, when the voltage at the substation was adjusted to the maximum value, the voltage rise criterion tended to be the most restrictive in HC maximization [11]. However, subject to an appropriate voltage state, the HC is limited by the conductor’s ampacity. Moreover, the maximum capacity is limited by the voltage rise, and the topology of lines is crucial for estimating the maximum capacity of the radial-feeder distributed generators [12]. Sun et al. [13] introduced harmonic distortion limits as new constraints for HC assessments. They identified the effects of total harmonic distortion and individual harmonic planning level limits when considering power quality as a performance index in HC estimation. In [14], a location-based individual feeder analysis for the HC of a PV-connected feeder was presented. This

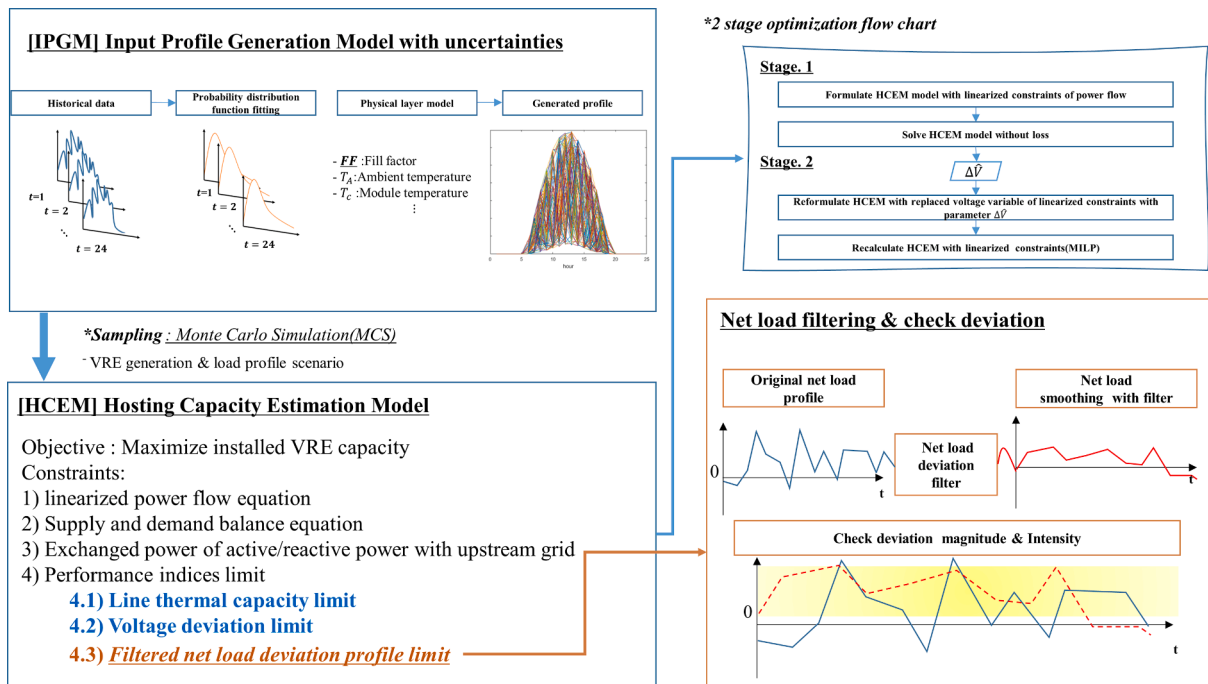


Fig. 1. Proposed HC framework considering net load deviation.

approach considers the correlation between the locations of installed PVs in a region. An increase in the VRE penetration rate complicates the protection system design. It was found that fluctuating wind power injection results in voltage disturbances and severe voltage flicker propagation at each node [15]. In [16], a relay protection coordination approach was presented. The method integrates optimal DG placement and sizing methods in accordance with the impact of the DG location and size on the fault current.

1.2.2. Hosting capacity's simulation method reviews

After choosing the performance indices, we must model the procedure for assessing the impact on the performance index as the penetration rate of VREs increases. A simple iterative approach exploits the weak sections of a remote feeder and specifies the potential of multiple voltage regulators on the long rural section that feeds power to remote communities [17]. However, this approach does not address the impact of simultaneous VRE deployment on other nodes. Additionally, this deterministic method cannot capture the VRE intermittent output power profile, which is a core factor determining HC. To overcome these limitations, a probabilistic HC analysis was investigated. The planning framework for the optimal mix of VRE in distribution networks was presented in [18]. In this framework, the probability distribution function was utilized to consider the uncertainties associated with solar and wind DGs. Moreover, in [6], a risk assessment tool-based probabilistic HC model was proposed. When modeling PV uncertainties, localized solar irradiances were considered with a detailed formulation of a clearness index that accurately characterized the locational weather conditions. Spatio-temporal probabilistic voltage sensitivity analysis was applied to exploit both spatial and temporal uncertainties associated with PV injections [19]. In [17], an estimation framework considering the time-series impact based on scenarios for PV capacity deployment was proposed. The correlations between wind speeds from adjacent sites on a wind farm were modeled using a probabilistic approach [20]. In [21], a process of lowering from a violation to a violation-free state was proposed, with the aim of mitigating the violations: nodes overvoltage, lines overcurrent, and transformer overloading in grid operation. In [22], a multi-period AC optimal power flow (OPF) approach was proposed based on HC estimation under active network management

schemes. However, this multi-period AC OPF was formulated with nonlinear programming, which requires high computational complexity.

1.3. Contributions

To narrow the gap between the DSO's reliable operation and TSO's securing system flexibility, this study proposed an HC estimation framework by expanding the HC problem from a distribution system-only problem to a problem considering coordinated operation with the transmission system's balancing responsibility. To this end, the volatility of net load, which has a great effect on the system's flexibility requirement, was included in the HC estimation model. In addition, the distribution system operation parameters, which were mainly considered in the existing HC estimation, were also encompassed without distortion. The HC results from the proposed study mitigate the variability in net load, allowing DSOs to fulfill their responsibilities for the operation of existing reliable distribution networks. Simultaneously, it reduces the cost of securing flexibility by alleviating the sudden variability of net load that occurs at the transmission-level. Finally, as a decision-making tool for DSO, it can be served as a cornerstone for various distribution system operations and planning problem. The proposed framework can help address system operation and planning problems by enabling decision makers to verify cost-effective HC without requiring further management of net load deviation due to the high-penetrated VREs.

From the above, the key contributions of this study are listed below:

- A novel HC estimation framework that considers the net load deviation as a new performance index was proposed to mitigate the abrupt net load deviation resulting from the VRE maximum penetration rate.
- By using a net load deviation filter that can be applied to all intervals based on a consistent criterion, the framework effectively captured the net load deviation intensity and magnitude without losing consistency in achieving conservative results.
- To identify the effectiveness of the proposed performance index, the results were compared with those of the conventional HC model, and

performance indices violation analysis was performed to verify key elements for improving HC.

- To consider the net load volatilities and uncertainties of VRE and loads, a multi-time stochastic optimization model was formulated.
- To evaluate the economic effect of the proposed model, the estimation of the accommodation costs for VREs was compared with the results of the conventional HC model.

The remainder of this paper is structured as follows. Section 2 introduces the proposed HC estimation framework, the input profile generation model based on a probabilistic approach, and the mathematical description of net load deviation. Section 3 describes the stochastic optimization model. Section 4 presents the numerical results of the net load deviation effect on HC (4.2.1), the qualification of the proposed index, and the verification of the key elements for improving hosting capacity (4.2.2). Accordingly, the ability to capture net load deviation is assessed. Section 5 provides the estimation of the VRE accommodation costs based on HC calculated by the proposed model. Section 6 concludes the paper.

2. HC estimation framework considering net load deviation.

This section describes the proposed HC estimation framework. Fig. 1 illustrates the HC estimation framework considering net load deviation. The proposed framework comprises an input profile generation model (IPGM) and a hosting capacity estimation model (HCEM), which include a net load filtering module. In the IPGM, probability distribution fitting is performed using historical data to consider the VRE uncertainties and loads. The input profile is generated based on the predefined physical characteristics of each resource and fitted probability function. The HCEM consists of two-stage optimization. The mathematical formulation of power flow in the distribution system is mainly expressed in a non-linear form, which acts as a major hindrance to solving optimization problems in a timely manner. To address this nonlinearity, this study utilized a linearization method based on several practical assumptions. In the first stage, an HC optimization model without loss is formulated with linearized power flow constraints. From the result of stage 1, ∇v can be obtained. In the second stage, the reformulated HC model including power flow's losses could be solved with replaced parameter ∇v . The detailed validation of the linearization is described in [23]. In addition, the net load deviation filter was modeled in the form of an HCEM constraint. A convolutional technique was used to effectively capture the magnitude and intensity of net load deviation for each period to evaluate deviation with a consistent criterion. Details are provided in Section 2.4. Finally, we obtained the maximum installed PV and WT for each node of the distribution grid with consideration of the net load deviation.

2.1. Load profile model

Electricity consumption is affected by various factors, such as weather, climate, and customer behavior [24]. In this study, a Gaussian distribution was used over time to reflect the pervasive characteristics of electricity consumption [25]. The Gaussian probability distribution function of the load can be expressed as follows:

$$PDF_{Demand}(P_t^D) = \frac{1}{\sqrt{2\pi}\sigma_{P_t^D}} e^{-\frac{1}{2}\left(\frac{P_t^D - \mu_{P_t^D}}{\sigma_{P_t^D}}\right)^2}, \forall t \quad (1)$$

where P_t^D represents the load at time t , $\mu_{P_t^D}$ is the mean of the load, and $\sigma_{P_t^D}$ is the standard deviation of the load.

2.2. Photovoltaic generation profile model

When modeling the probability distribution function of solar irra-

diance to characterize the uncertainty of irradiance, it can be assumed that irradiance follows a beta probability distribution function [26], which can be expressed as.

$$PDF_{PV}(irr_t) = \frac{\Gamma(\alpha_t + \beta_t)}{\Gamma(\alpha_t)\Gamma(\beta_t)} (irr_t)^{\alpha_t-1} \cdot (1 - irr_t)^{\beta_t-1}, \forall t \quad (2)$$

(For $\alpha_t, \beta_t > 0$, $0 < irr_t < 1$),

where irr_t is a random variable for solar irradiance over time t . The probability density function of beta is defined when the value of the random variable lies between 0 and 1. To fit the probability density function and obtain its parameters, the irradiance values of the beta distribution over time are scaled before fitting via normalization. Γ denotes the gamma function, and α_t and β_t are the gamma function shape parameters. The shape parameters are determined by the average and variance of solar irradiance for each time segment, as follows:

$$\alpha_t = \frac{\mu_{irr_t} \cdot \beta_t}{(1 - \mu_{irr_t})}, \beta_t = (1 - \mu_{irr_t}) \cdot \left(\frac{\mu_{irr_t} (1 + \mu_{irr_t})}{\sigma_{irr_t}^2} \right) - 1 \forall t \quad (3)$$

The output of a PV unit is mainly affected by the characteristics of its module, solar irradiance, and the ambient temperature of the site. Therefore, the expected output of solar power can be expressed as in (4) – (8), given the meteorological conditions, including solar irradiation and the module characteristics [27]. The V–I characteristic curve, which is the main component affecting the PV module output, can be determined for a given radiation level and ambient temperature (T_A) using the following equations [28]:

$$PG^{PV}(irr_t) = N_{PV_{mod}} \cdot FF \cdot V_g \cdot I_g \quad (4)$$

$$I_g = I_{SC} + K_i(T_C - 25) \quad (5)$$

$$T_C = T_A + S \left(\frac{N_{OT} - 20}{0.8} \right) \quad (6)$$

$$V_g = V_{OC} - k_v \cdot T_C \quad (7)$$

$$FF = \frac{V_{MPP} \cdot I_{MPP}}{V_{OC} \cdot I_{SC}} \quad (8)$$

where $N_{PV_{mod}}$ is the total number of PV modules, $PG^{PV}(irr_t)$ is the PV generation output; FF represents the fill factor, T_A and T_C are the ambient and module temperatures, respectively, K_v and K_i are the voltage and current temperature coefficients, respectively, N_{OT} is the nominal operating temperature of the cell, I_{SC} and V_{OC} indicate the short-circuit current and open-circuit voltage, respectively, and I_{MPP} and V_{MPP} denote the current and voltage respectively, at the maximum power point.

2.3. Wind turbine generation profile model

Wind speed variability is known to be the main factor contributing to the uncertainty in wind power generation. The Rayleigh and Weibull probability distribution functions have been typically used to represent the stochastic behavior of wind speed [29]. In this study, the Weibull distribution function was employed to describe the wind speed variability and uncertainty. Wind speed is modeled as a random variable over each period following the Weibull probability distribution function with parameters λ_t (scale factor) and π_t (shape parameter), which are expressed as.

$$PDF_{wind\ speed}(w_t) = \frac{\pi_t}{\lambda_t} \left(\frac{w_t}{\lambda_t} \right)^{\pi_t-1} e^{-\left(\frac{w_t}{\lambda_t} \right)^{\pi_t}} \forall t (w_t > 0, \lambda_t > 1, \pi_t > 0) \quad (9)$$

$$\pi_t = \left(\frac{\sigma_{w_t}}{\mu_{w_t}} \right)^{-1.086} \forall t \quad (10)$$

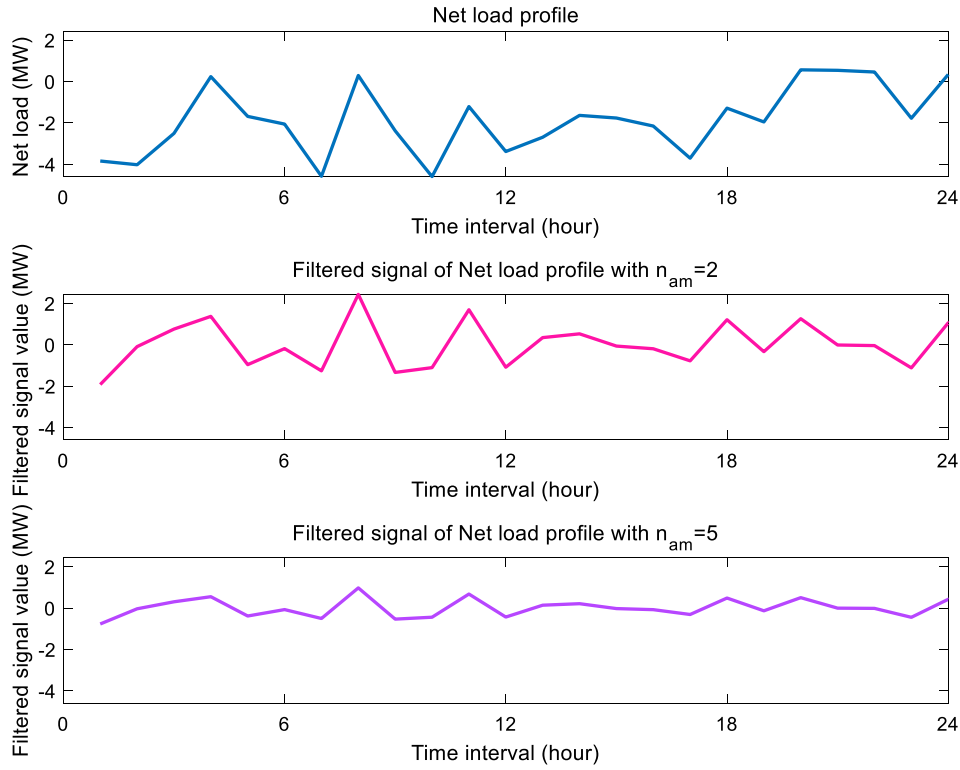


Fig. 2. Example of net load profile and filtered profile for each n_{am} parameter.

$$\lambda_t = \frac{\mu_{w_t}}{\Gamma\left(1 + \frac{1}{\pi_t}\right)} \forall t \quad (11)$$

where μ_{w_t} and σ_{w_t} represent the mean and standard deviation of the wind speed at time t , respectively, and λ_t and π_t represent the scale factor and shape parameter at time t , respectively.

The output of a WT generator unit can be expressed using the generator power performance curve [18]. For the polynomial characteristics of the power performance curve, the output of the WT generator at the wind speed can be calculated as.

$$P^{WT}(w_t) = \begin{cases} aw_t^3 + bP_{rated}^{WT}, & w_{cut-in} \leq w_t < w_n \\ P_{rated}^{WT}, & w_n \leq w_t < w_{cut-out} \\ 0, & otherwise \end{cases} \quad (12)$$

$$a = \frac{P_{rated}^{WT}}{(w_n^3 - w_{cut-in}^3)} \quad (13)$$

$$b = \frac{w_{cut-in}^3}{(w_n^3 - w_{cut-in}^3)} \quad (14)$$

where P_{rated}^{WT} represents the rated power that can be generated by WT, and $w_{cut-out}$ represents the cut-out wind speed. Meanwhile, a and b are calculated by the cut-in wind speed (w_{cut-in}) and nominal wind speed (w_n).

2.4. Net load deviation filter

This section introduces several definitions of net load deviation. Definition 3 used in the proposed model was described in terms of comparison with Definitions 1 and 2. The net load typically refers to the combined variability in power consumption and non-dispatchable generation [30]. At the subsystem level in the distribution grid, the net load is defined as the power flow measured at the feeder head substation in the distribution network [31,32]. Because this study focuses on the

description of the variability of the net load in the distribution system, which is directly connected to VRE, the net load referenced herein adheres to the latter definition. Similarly, the net load deviation indicates the change rate of the net load within a specified time interval. The net load deviation can be characterized according to three features: (1) direction, including upward (+) and downward (-) deviation; (2) magnitude, which can be defined as the deviation start time – the deviation end time; and (3) duration: the time interval between the deviation start and end times. With these three features, referring to [33], the net load deviation can be described mathematically as follows:

Definition 1

$$|NL(t + \Delta t) - NL(t)| \geq NLD_{val} \forall t \quad (15)$$

where $NL(t)$ represents the net load at time t and NLD_{val} and Δt denote the predefined threshold value and user-defined time-duration parameter, respectively.

From Definition 1, we can obtain the net load deviation by calculating the difference between the start and end values for a predefined duration. This value can be considered for both upward/downward directions of the abrupt net load deviation. However, Definition 1 cannot consider the net load deviation that occurs within a predefined duration.

Definition 2

$$\max(NL[t, t + \Delta t]) - \min(NL[t, t + \Delta t]) \geq NLD_{val} \forall t \quad (16)$$

In contrast to Definition 1, Definition 2 calculates the net load deviation by considering only the maximum and minimum values among all net load values within the predefined duration. Using Definition 2, we can obtain the magnitude of fluctuations within a predefined duration. However, this method does not consider the net load profile slope, which is the change rate over the differences in net load deviation.

Definition 3.

$$NLD_t^f = \text{mean}\{NLD_{t+h} - NLD_{t+h-n_{am}}; h = 1, \dots, n_{am}\}, \\ = NLD_t \cdot f_{n_{am}}$$

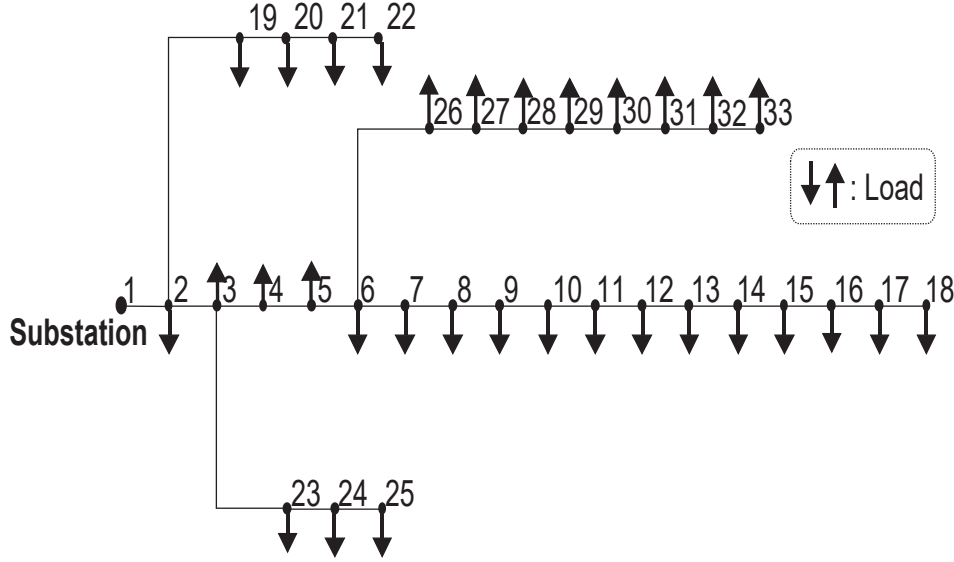


Fig. 3. IEEE 33-radial bus system.

$$NLD_t^f = \frac{1}{n_{am}} \sum_{h=1}^n NLD_{t+h} - \frac{1}{n_{am}} \sum_{h=1}^n NLD_{t+h-n} \quad (17)$$

where n_{am} represents the number of average differences of measured values as in (15). In Definition 3, the net load profile is considered a signal. Herein, NLD_t^f represents the variation in the initial net load profile, which is represented by NLD_t . Note that NLD_t^f can be expressed as a convolution product of the net load profile with $f_{n_{am}}$. The number of averaged measures, n_{am} , denotes the width of $f_{n_{am}}$ to be considered as a smoothing filter. For example, a small value of n_{am} makes the filtered profile NLD_t^f more sensitive to a short-time-interval deviation of the net load, NLD_t .

Fig. 2 illustrates the effects on the n_{am} parameters. According to Definition 3, the length of the filtered signal can be shorter or longer than the length of the original signal, depending on time band parameter n_{am} . In addition, the filtered signal is not a net load in the physical sense because it has been reprocessed by smoothing and differentiating processes. In terms of limiting the value of net load deviation as the VRE capacity increases, Definition 3 has several advantages when considering the net load volatility in the HC estimation model. It effectively accounts for both the magnitude and intensity of the net load deviation. Particularly, when setting the performance index limit for the net load deviation, it can be equally applied at the level of deviation intensity and magnitude for the global time horizon with a consistent criterion. Thus, the characteristics of Definition 3 appear to be effective in considering the HC net load deviation problem. Thus, Definition 3 was used to formulate the optimization problem.

3. Problem formulation considering net load deviation.

In this study, the stochastic optimization problem was developed based on mixed-integer linear programming (MILP), and it was expanded to a multi-time formulation to reflect the uncertainty and intermittency of VRE and the temporal effect. Moreover, the complexity of the multi-time period can be easily addressed by integrating the iteration process, which is a time-consuming step, with the optimization problem.

Objective function.

The objective function of HC estimation maximizes the capacity of WT and PV that can be installed for all nodes. This can be expressed as follows:

$$\text{Maximize } \sum_{\forall i} (C_i^{PV} + C_i^{WT}) \quad (18)$$

where C_i^{PV} and C_i^{WT} can be determined by the generation profile of each generator, bus voltage magnitudes and angles, real and reactive line flows, and real and reactive power exchanges with the upstream grid.

Constraints.

The proposed optimization model should satisfy certain equality and inequality constraints described below.

Linear power flow.

Equations (19) and (20) represent the active and reactive power flows of the line, respectively, which are linearized according to the assumptions. $\Delta \widehat{V}_{i,t}$ can be obtained from the lossless optimization problem. The installed number of unit PV and WT variables is a free positive variable in all nodes, except the point of the interconnection node.

$$PL_{ij,t} = g_{ij}(1 + \Delta \widehat{V}_{i,t})(\Delta V_{i,t} - \Delta V_{j,t}) - b_{ij}(\Delta \theta_{i,t} - \Delta \theta_{j,t}) \forall ij, \forall t \quad (19)$$

$$QL_{ij,t} = -b_{ij}(1 + \Delta \widehat{V}_{i,t})(\Delta V_{i,t} - \Delta V_{j,t}) - g_{ij}(\Delta \theta_{i,t} - \Delta \theta_{j,t}) \forall ij, \forall t \quad (20)$$

Active/reactive supply and demand balance.

Constraints (21) and (22) ensure that the sum of the active and reactive powers of the VRE power installed in each node and that from all lines connected to the node is equal to the load at that particular node. In addition, $P_t^{PV_{gen}}$ and $P_t^{WT_{gen}}$ are the output of per unit PV and WT calculated by the IPGM of the framework presented in Sections 2.2 and 2.3. Here, set B is a subset of i . Further, $P_{c,t}^M$ and $Q_{c,t}^M$ are assigned values only when there is a point of interconnection connected to node i .

$$\sum_{c \in C_i} P_{c,t}^M + \sum_{i \in L_i} PL_{ij,t} + P_t^{PV_{gen}} \bullet C_i^{PV} + P_t^{WT_{gen}} \bullet C_i^{WT} = P_{i,t}^D \forall i \in B, C_i \subset B \quad (21)$$

$$\sum_{c \in C_i} Q_{c,t}^M + \sum_{i \in L_i} QL_{ij,t} + Q_t^{PV_{gen}} \bullet C_i^{PV} + Q_t^{WT_{gen}} \bullet C_i^{WT} = Q_{i,t}^D, \forall i \in B, C_i \subset B \quad (22)$$

Active/reactive power exchange with upstream grid limit.

Constraints (23) and (24) limit the amount of active and reactive power that can be exchanged with the upstream grid, considering the

Table 1
Specification of PV modules and WT [35].

Power	Parameter	Value	
PV	P_{rated}^{PV}	220 [KW]	
	V_{oc}	36.96 [V]	
	I_{sc}	8.38 [A]	
	V_{MPP}	28.36 [V]	
	I_{MPP}	7.76 [A]	
	k_i	0.0054 [A/°C]	
	k_v	0.1278 [V/°C]	
	N_{OT}	43 [°C]	
	Wind	P_{rated}^{WT}	250 [kW]
		w_{cut-in}	3 [m/s]
$w_{cut-out}$		25 [m/s]	
w_n		12 [m/s]	

main substation feeder capacity.

$$-P_c^{M,max} \leq P_{c,t}^M \leq P_c^{M,max} \forall c, \forall t \quad (23)$$

$$-Q_c^{M,max} \leq Q_{c,t}^M \leq Q_c^{M,max} \forall c, \forall t \quad (24)$$

Performance indices limit.

The performance indices include the line capacity, node overvoltage, and net load deviation. To avoid violating these performance indices, constraints (25)–(29) establish upper and lower limits on the deviation of the voltage magnitude, as well as the real and reactive power flows of lines, respectively. In addition, constraint (29) represents the maximum net load deviation for NLD_i^f . Specifically, it limits the amount of variation and intensity in the filtered profile of the net load owing to the installed capacity of the VRE generation profile and load.

$$-PL_{ij}^{max} \leq PL_{ij,t} \leq PL_{ij}^{max} \forall ij, \forall t \quad (25)$$

$$-QL_{ij}^{max} \leq QL_{ij,t} \leq QL_{ij}^{max} \forall ij, \forall t \quad (26)$$

$$V_{i,t} = 1 + \Delta V_{i,t} \forall i, \forall t \quad (27)$$

$$-V^{max} \leq V_{i,t} \leq V^{max} \forall i, \forall t \quad (28)$$

$$P_{c,t}^M \bullet f_{nam} \leq NLDI^{max} \forall c, \forall t \quad (29)$$

4. Numerical results

The proposed HC estimation framework was applied to an IEEE 33-radial bus system [34]. The bus, line number, and line capacity are specified in Appendix A. The proposed framework was implemented in MATLAB and tested on a desktop with an Intel Core i9-10900 K 3.7 GHz processor. The MILP problem was solved through MATLAB Optimization Toolbox and the average simulation time was 1.043 s. To demonstrate the proposed model, comparative studies were analyzed: (1) base case: HC estimation without considering the net load deviation, and (2) test case: the proposed estimation model. Based on the stochastic approach, 500 repetitions were performed using Monte Carlo simulation (MCS).

4.1. Test system parameters and generation profiles

The IEEE 33-bus distribution system, illustrated in Fig. 3, was used to test the proposed framework. The system nominal voltage was 12.66 kV and substation node 1 was considered the point of interconnection where the voltage was assumed to be 1 [p.u.]. The proposed framework was implemented using the Southern California Edison (SCE) hourly dynamic load profiles of domestic single/multiple customers [36]. The historical solar irradiation, that is, the global horizontal irradiation and wind speed data along latitude: 37.73 and longitude: -122.50, where SCE was responsible for supplying electricity, were obtained from the NREL National Solar Radiation Database (NSRDB) [37]. NSRDB provides solar radiation and meteorological data for the United States and regions of the surrounding countries. The technical characteristics of PV and WT are specified in Table 1. The PV and WT plants in Table 1 refer to the specifications of the reference unit PV and WT. Based on these data, the mean profiles of the load, unit PV, and WT generated by the IPGM are shown in Fig. 4.

4.2. Comparative analysis

In the performance indices of the proposed model, the voltage deviation was set to 0.95–1.05 [p.u] according to ANSI C84.1–2016 [38]. In the test case, the net load deviation parameter was set to be 20 % of the maximum line capacity of the test system. Conventionally, the VRE ramping event is considered to be 20 % of the installed capacity. The

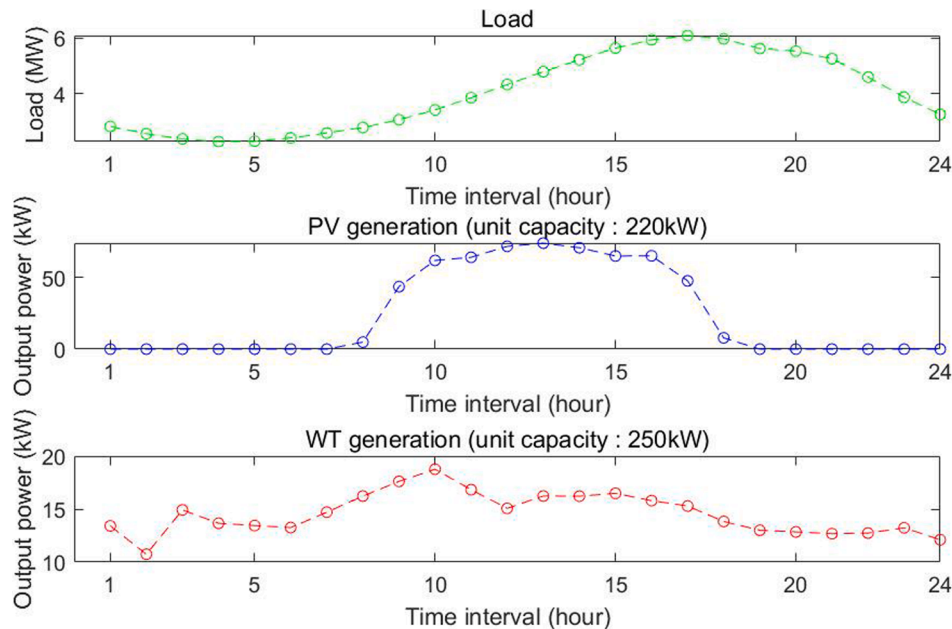


Fig. 4. Average profiles of load, unit PV, and unit WT.

Table 2
Hosting capacity results (mean values) of base case and test cases.

Label	Hosting capacity [MW]	Installed PV capacity [MW]	Installed WT capacity [MW]
Base case	22.88	5.22	17.67
Case 1 (Time band(n_{am}) = 2h)	9.88	2.74	7.14
Case 2 (Time band(n_{am}) = 3h)	14.84	4.06	10.78
Case 3 (Time band(n_{am}) = 4h)	19.13	5.05	14.08

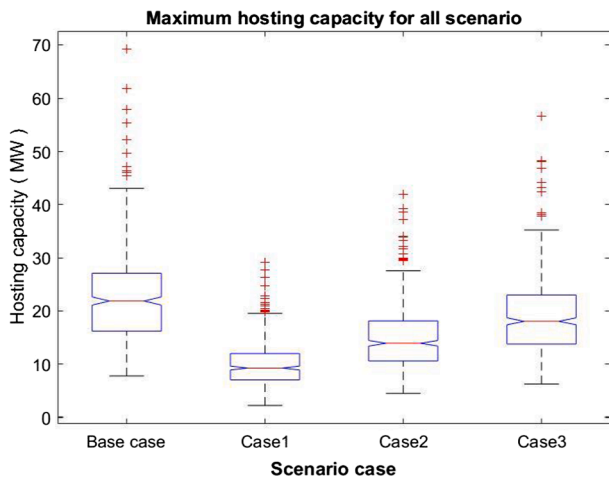


Fig. 5. Box and whisker plot of HC results.

average HC based on the use of MCS (500 iterations) is summarized in Table 2. The best and worst scenarios are the cases with the highest and lowest hosting capacities with respect to the number of repetitions, respectively. The rated capacities of the PV and WT used in this study were 220 kW and 250 kW, and the efficiencies calculated based on the scenario results were 10.3 % and 4.1 % on average, respectively.

4.2.1. Net load deviation effect on HC

Table 2 indicates that the installed WT capacity in the base and test cases account for a high proportion of the HC. These results can be attributed to the different characteristics of the VRE generation profiles. They are influenced by regional meteorological characteristics and seasonality. Considering this effect, the most robust estimation result of hosting capacity was 22.98 MW, which was negligibly similar to the results shown in Table 2. The relatively high HC results in the base case were due to the harsh environment of the test system for WT operation. Generally, regions with a minimum wind speed of 5.8 m/s or higher are considered for WT investment, but our test system environment is in a

region with an average wind speed of less than 3 m/s, 48 % of the time, which means that WT with a cut-in rate of 3 m/s cannot guarantee sufficient power generation [39]. This results in a more than twofold difference in HC. This suggests that, from the perspective of renewable energy generators, the correlation between the HC results from the proposed model and the operating environment can be used as a quantitative indicator that helps the feasibility of renewable energy investment and pre-investment decision-making. In the maximization of the HC problem, WT, which has a relatively uniform power generation output over 24 h when compared to PV, can be considered a more attractive resource than PV. Fig. 5 depicts the HC results and their variance for each case from MCS. For the test case, as the value of the time band (n_{am}) decreases the box mean value and whisker length (HC variance) tend to decrease. This implies that, when the variability of the net load is strictly considered, the HC is estimated conservatively with lower capacity than the base case for the extreme input profile case. It also implied that the proposed model reacts sensitively to minimal net-load deviation intensities. From the results, DSO must determine the appropriate HC by considering the trade-off between the level of variability in HC and netload deviation.

4.2.2. Performance indices violation analysis: Key element for improving HC and qualification of net load deviation index

In this subsection, performance indices violations are analyzed for the generated scenario. Violations are confirmed for three performance indices: voltage regulation, line capacity, and net load deviation. For the net load deviation violation, the violation of the filtered signal according to definition 3 of Section 2 was applied. Two or more violations can occur simultaneously for the multi-time horizon (24 h) of each scenario. The violation results are presented in Table 3. Of the three indices, line capacity and voltage violation have a decisive influence on HC for almost all scenarios. A potential concern when using a novel criterion is whether the HC is drastically affected by the proposed index. If the HC is highly dependent on the proposed index limit, it may distort the HC. However, it was confirmed that the proposed index is considered accordant without distorting the effect of the conventional performance index on HC. Fig. 6 shows the resulting voltage violation for nodes and time periods by heat map. It is observed that the more frequently the voltage violation occurred, the brighter the color, and vice versa. In the case of the voltage deviation, the violation frequently occurs in nodes 23–25. In node 23, it is confirmed that the voltage violation occurs most of the time, whereas in the case of node 24 there is scarcely a violation. In the case of node 23, voltage upper limit violation mainly occurs during the daytime period, which is due to an oversupply of PVs. No voltage violation occurs on any bus other than the 23–25 nodes, which suggests that DSO may effectively improve the HC by managing only a few major buses. Fig. 7 shows the results of line capacity violation for every line of the network and period. The line capacity violation mainly occurs on lines 22–25, which are connected to violated voltage nodes 23–25, and nodes 26–30, which are the other branch nodes extending from the main feeder. Moreover, it is shown that lines 17–21 are low-usage lines that have no capacity violation in any case. As in the case of voltage violations, it is observed that most line capacity violations

Table 3
Performance indices violation results for each scenario.

Performance index Case	Performance indices					
	Voltage deviation		Line capacity		Net load deviation (Definition 3)	
	Upper limit violation	Lower limit violation	Upper limit violation	Lower limit violation	Upper limit violation	Lower limit violation
Base case	100 %	92.8 %	100 %	96.2 %	–	–
Case 1	–	88 %	–	96.2 %	11 %	12.6 %
Case 2	–	95.6 %	–	96.2 %	15.6 %	17.8 %
Case 3	–	95.6 %	–	96 %	22.2 %	22.2 %

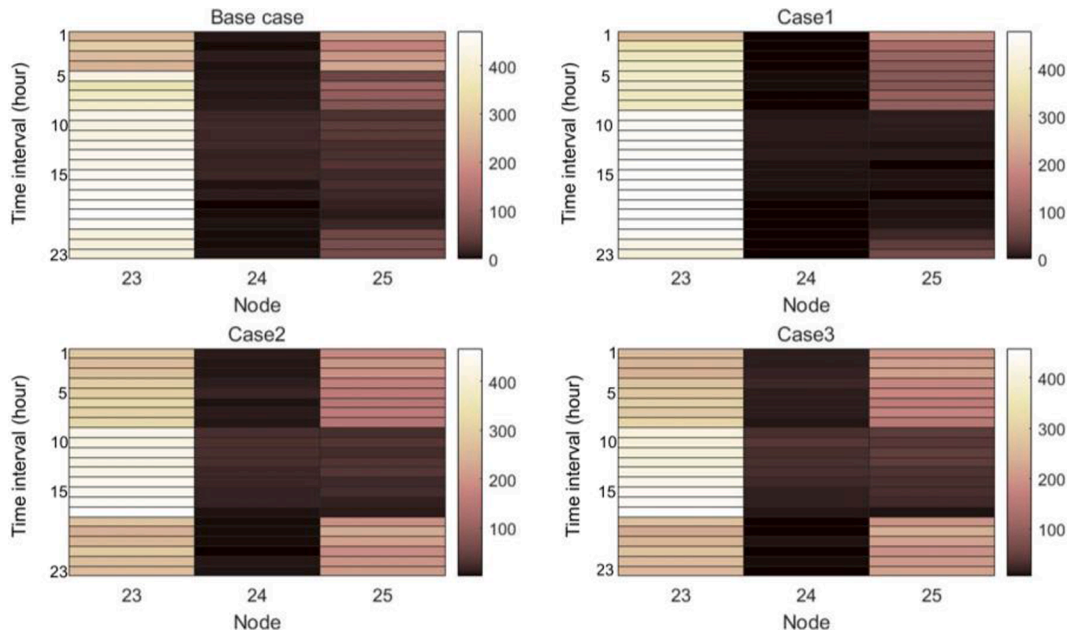


Fig. 6. Voltage deviation violation heat maps.

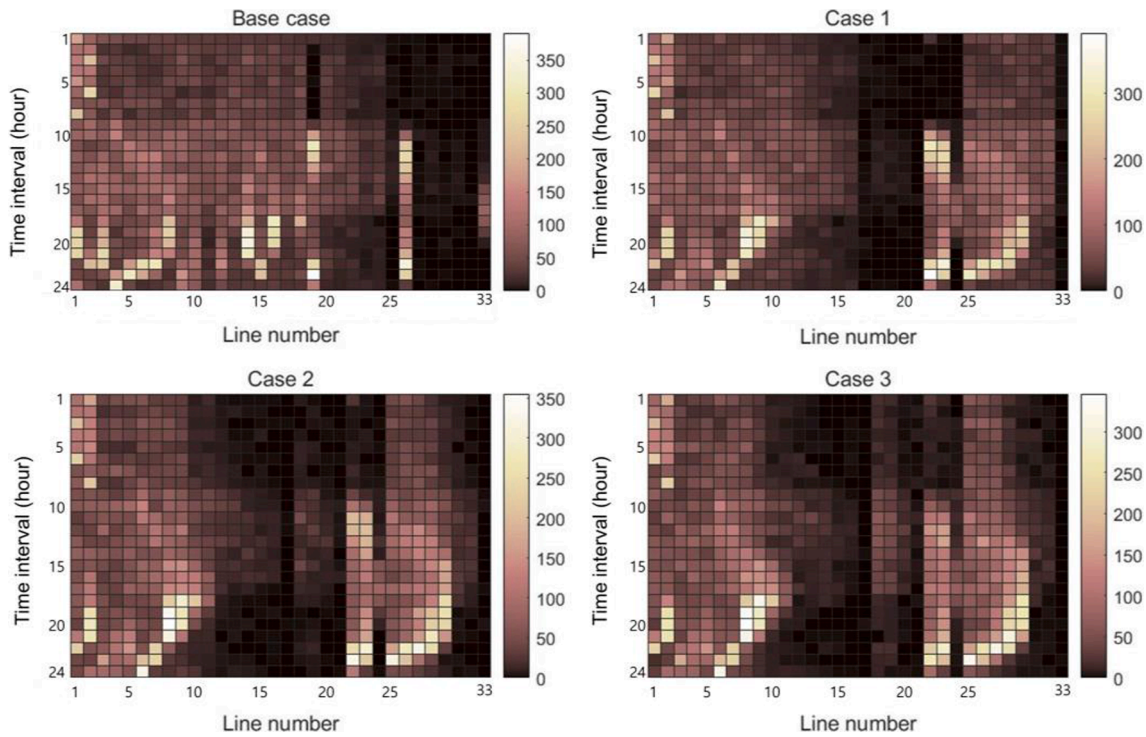


Fig. 7. Line capacity violation heat maps.

occurred in a few major lines connected to frequently violated nodes.

Based on the above results, it was confirmed that there were a few specific lines and buses that hindered the HC improvement, and it was closely related to the network topology. Moreover, during the period in which the violation occurred, the DSO could proactively prepare for periods when flexibility was required.

4.2.3. Performance indices violation analysis: Capturing net load variability

To validate the effectiveness of the net load deviation filter, the net load variability was analyzed in terms of intensity and magnitude. In

Fig. 8, the intensity of the net load deviation according to the time band parameters is identified. In Fig. 8 (a) and (c), the net load profile of case 3 is almost identical to that of the base case. In contrast, in Fig. 8(b) and (d), the net load profile of case 1, which is the strictest case for net load deviation, shows a significant decrease in the net load intensity compared to the base case over the time horizon.

Table 4 summarizes the variability in terms of the magnitude of net load deviation for all cases in the worst and best scenarios. From Fig. 8 and Table 4, the effectiveness of the proposed index in capturing the net load deviation magnitude and intensity is verified. This implies that the proposed performance index can effectively detects volatility in the net

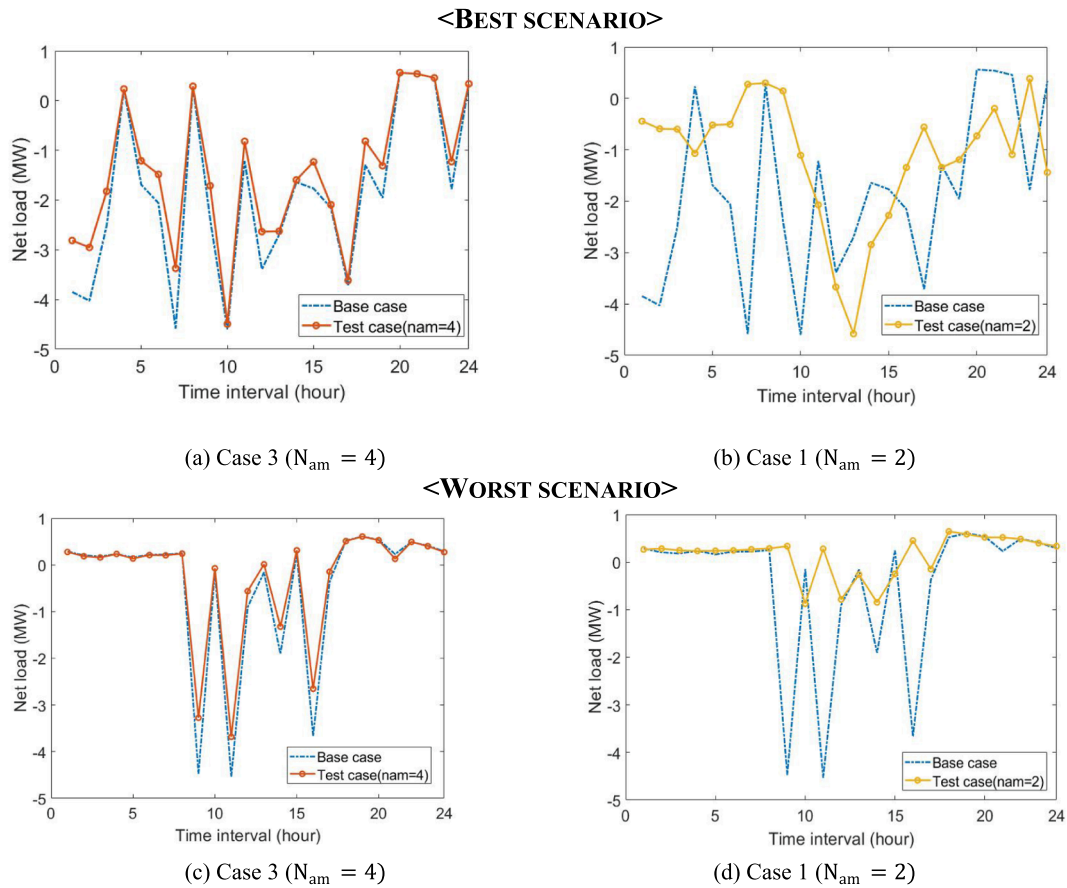


Fig. 8. Net load profile for the test case 1 and 3.

Table 4
Summary of total net load deviation magnitudes resulting from each case.

Case	Worst scenario[MW]	Best scenario[MW]
Base case	31.06	38.28
Case 1 (Time band(n_{am}) = 2h)	7.71	17.02
Case 2 (Time band(n_{am}) = 3h)	17.8	24.56
Case 3 (Time band(n_{am}) = 4h)	24.68	33.16

Table 5
Conventional generator parameters [40].

	Nuclear	Coal	CC	CT
Annual Investment cost [k\$/MW/year]	224.00	174.72	60.12	38.52
Fixed cost [k\$/MW/year]	89.88	30.04	14.58	14.88
variable cost (\$/MWh)	6.5	19.05	39.80	53.78
Start up/ shut down cost (\$/MW/start)	N/A	150	50	15

load resulting from the maximum HC.

5. Discussion: Estimation of the accommodation costs for VREs

In this section, the VRE accommodation cost is calculated according to the method in [41] based on the power system economics theory. The accommodation cost has been defined as the “additional cost of

accommodating wind and solar” [42]. This cost can be estimated by comparing two power system states, with and without VRE, to separate the additional system costs. To evaluate the economic effect on HC, the accommodation costs of VRE were compared based on the HC result calculated by the test case and base case. It is assumed that the entire system is composed of a set of identical distribution systems and the proposed HC is applied in all of them respect to each load level. The LDC is calculated based on the California independent system operator EMS load data. The conventional generator parameters for annual fixed costs and variable costs are shown in Table 5. The accommodation costs can be categorized into balancing costs, grid costs, and profile costs. The balancing costs are related to the uncertain VRE supply. The grid costs reflect the network expansion cost according to the distance between the VRE and the load, and the increased re-dispatch costs of conventional generators for congestion management. The profile costs are incurred by VRE variability. As this analysis focuses on the net load deviation effect, the profile costs related to the volatility of the net load are analyzed. For more information on modeling balancing costs and grid costs, see [43]. Fig. 9 shows the load duration curve (LDC) of the entire power system and the screening curve. From Fig. 9 and Table 5, we can recalculate Fig. 10, which is the reduced load duration curve (RLDC). As illustrated in that figure, the profile cost caused by the variability of VRE is expressed as low-capacity credit and the reduced full-load hour. Finally, the profile costs can be calculated by integrating along the inverse RLDC and multiplying every full-load hour value with the respective minimal screening curve value. Table 6 summarizes the results of the HC accommodation cost for base and test cases. It can be confirmed that the more strictly considered the constraints on the net load deviation volatility are, the lower the accommodation cost. In particular, in the base case without consideration of net load deviation in base case, the full-load hour reduction cost comprises a notable portion of the

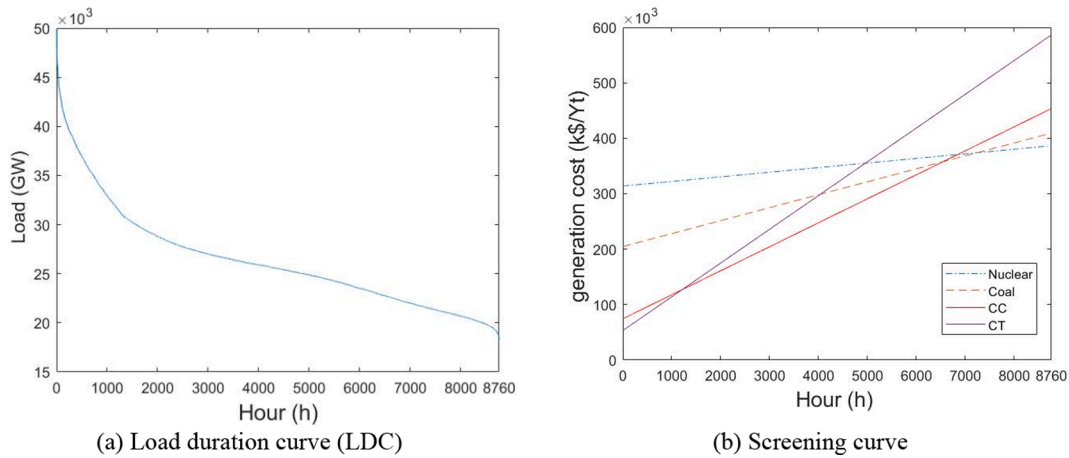


Fig. 9. Load duration curve (LDC) (a) and Screening curve(b).

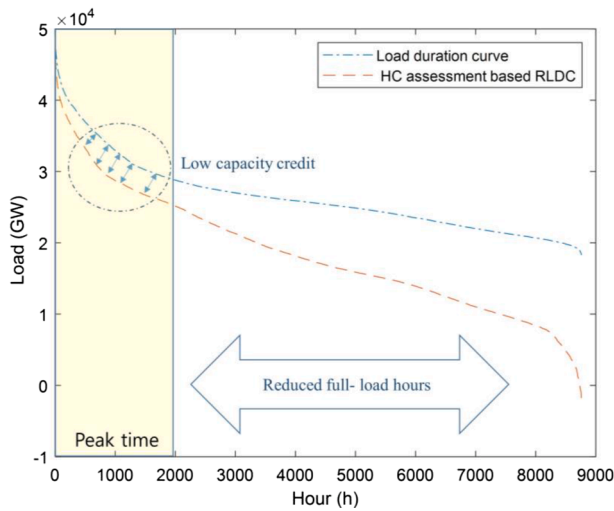


Fig. 10. Example of Load duration curve and HC assessment based reduced load duration curve (RLDC).

Table 6
VRE accommodation costs results.

Case	Accommodation cost (profile cost only) [\$/MWh]	Back-up cost [\$/MWh]	Full load hour reduction cost [\$/MWh]
Base case	9.17	1.40	7.78
Case 3	9.10	1.72	7.37
(Time band (n _{am}) = 4h)			
Case 1	8.68	3.37	5.31
(Time band (n _{am}) = 2h)			

accommodation cost. On the other hand, in the test case, it was confirmed that the full load hour reduction cost caused by net load variability appeared less than the base case. Based on the above results, the system operators could determine an appropriate HC according to their own environment. However, it should be notice that this is the cost when VREs are penetrated to the entire system. Therefore, it appears reasonable to regard it as the minimum cost for accommodating VREs.

6. Conclusion

In this study, a novel HC estimation framework was designed that considers the net load deviation as a performance index with technical parameters (i.e., over voltages and ampacity). The proposed framework was formulated via MILP based on considerations of multiple periods under VRE and load uncertainties within a short duration. To validate the proposed model, net load deviation effects on HC were analyzed (Section 4.2.1). In Section 4.2.2, the qualification of the proposed net load deviation component as a new performance index and key elements for improving HC was verified. The proposed net load deviation filter exhibited excellent detection ability for net load deviation, as shown in Section 4.2.3. Finally, as an application of the proposed model to help the system operator’s precise decision making, the VRE accommodation costs were analyzed in a highly VRE penetrated system. Thus, the proposed model is expected to serve as a decision-making tool for system operators when considering planning and operation problems, such as, estimating system integration costs for ensuring system flexibility, TSO-DSO coordination, HC enhancement strategies for over-supply problem by utilizing EV fleets or heat pumps and network reconfiguration owing to an increase in the penetration level of VRE.

For the advancement of the proposed estimation framework, sophisticated modeling of its input profile generation is required with actual generation data based on data analytic approaches. To overcome the inconsistency problem of time resolution and consider the relationship between the regional characteristics and periodic variability, data-driven HC estimation models with key influencing factors through correlation analysis should be developed. Moreover, from a technological-economic point of view, further quantitative analysis research, such as system flexibility analysis, is needed.

Declaration of Competing Interest

The authors declare that they have no known competing financial interests or personal relationships that could have appeared to influence the work reported in this paper.

Data availability

Data will be made available on request.

Acknowledgements

This work was supported by the Korea Institute of Energy Technology Evaluation and Planning (KETEP) and the Ministry of Trade, Industry & Energy (MOTIE) of the Republic of Korea (No.

20226210100020 and No. 20192010106990).

Appendix A. IEEE 33 bus radial distribution bus and network data

From bus	To bus	Line number	Maximum line capacity (reactive power [KW])	Maximum line capacity (reactive power [KVAR])
1	2	1	4600	4600
2	3	2	4100	4100
3	4	3	2900	2900
4	5	4	2900	2900
5	6	5	2900	2900
6	7	6	1500	1500
7	8	7	1050	1050
8	9	8	1050	1050
9	10	9	1050	1050
10	11	10	1050	1050
11	12	11	1050	1050
12	13	12	500	500
13	14	13	450	450
14	15	14	300	300
15	16	15	250	250
16	17	16	250	250
17	18	17	100	100
2	19	18	500	500
19	20	19	500	500
20	21	20	210	210
21	22	21	110	110
3	23	22	1050	1050
23	24	23	1050	1050
24	25	24	500	500
6	26	25	1500	1500
26	27	26	1500	1500
27	28	27	1500	1500
28	29	28	1500	1500
29	30	29	1500	1500
30	31	30	500	500
31	32	31	500	500
32	33	32	100	100

References

- [1] International Energy Agency. Net Zero by 2050, <https://www.iea.org/reports/net-zero-by-2050>; 2021 [Online].
- [2] Koirala A, Van Acker T, D'Hulst R, Van Hertem D. Hosting capacity of photovoltaic systems in low voltage distribution systems: a benchmark of deterministic and stochastic approaches. *Renew Sustain Energy Rev* 2022;155:111899. <https://doi.org/10.1016/j.rser.2021.111899>.
- [3] Soroudi A, Rabiee A, Keane A. Distribution networks' energy losses versus hosting capacity of wind power in the presence of demand flexibility. *Renew Energy* 2017; 102:316–25. <https://doi.org/10.1016/j.renene.2016.10.051>.
- [4] Sakar S, Balci ME, Abdel Aleem SHE, Zobaa AF. Integration of large-scale PV plants in non-sinusoidal environments: considerations on hosting capacity and harmonic distortion limits. *Renew Sustain Energy Rev* 2018;82:176–86. <https://doi.org/10.1016/j.rser.2017.09.028>.
- [5] Chapaloglou S, Nesiadis A, Iliadis P, Atsonios K, Nikolopoulos N, Grammelis P, et al. Smart energy management algorithm for load smoothing and peak shaving based on load forecasting of an island's power system. *Appl Energy* 2019;238: 627–42. <https://doi.org/10.1016/j.apenergy.2019.01.102>.
- [6] Al-Saadi H, Zivanovic R, Al-Sarawi SF. Probabilistic hosting capacity for active distribution networks. *IEEE Trans Ind Inform* 2017;13:2519–32. <https://doi.org/10.1109/TII.2017.2698505>.
- [7] Birk, M, Chaves-Avila J. P, Gómez T and Tabors R. TSO/DSO Coordination In A Context of Distributed Energy Resource Penetration. MIT CEEPR Working Paper 2017-017.
- [8] Khoshjahan M, Dehghanian P, Moeini-Aghtaie M, Fotuhi-Firuzabad M. Harnessing ramp capability of spinning reserve services for enhanced power grid flexibility. *IEEE Trans Ind Appl* 2019;55(6):7103–12.
- [9] Ehsan A, Yang Q. State-of-the-art techniques for modelling of uncertainties in active distribution network planning: a review. *Appl Energy* 2019;239:1509–23.
- [11] Shayani RA, de Oliveira MAG. Photovoltaic generation penetration limits in radial distribution systems. *IEEE Trans Power Syst* 2011;26:1625–31. <https://doi.org/10.1109/TPWRS.2010.2077656>.
- [12] Papaioannou IT, Purvins A. A methodology to calculate maximum generation capacity in low voltage distribution feeders. *Int J Electr Power Energy Syst* 2014; 57:141–7. <https://doi.org/10.1016/j.ijepes.2013.11.047>.
- [13] Sun W, Harrison GP, Djokic SZ. Incorporating harmonic limits into assessment of the hosting capacity of active networks. In: CIREN 2012 Workshop. Integr Renew Distrib Grid. 2012.
- [14] Rylander M, Smith J, Sunderman W. Streamlined method for determining distribution system hosting capacity. *IEEE Trans Ind Appl* 2016;52:105–11. <https://doi.org/10.1109/TIA.2015.2472357>.
- [15] Sharma SK, Chandra A, Saad M, Lefebvre S, Asber D, Lenoir L. Voltage flicker mitigation employing smart loads with high penetration of renewable energy in distribution systems. *IEEE Trans Sustain Energy* 2017;8:414–24. <https://doi.org/10.1109/TSTE.2016.2603512>.
- [16] Zhan H, Wang C, Wang Y, Yang X, Zhang X, Wu C, et al. Relay protection coordination integrated optimal placement and sizing of distributed generation sources in distribution networks. *IEEE Trans Smart Grid* 2016;7:55–65. <https://doi.org/10.1109/TSG.2015.2420667>.
- [17] Abad MSS, Ma J, Zhang D, Ahmadyar AS, Marzooghi H. Probabilistic assessment of hosting capacity in radial distribution systems. *IEEE Trans Sustain Energy* 2018;9: 1935–47. <https://doi.org/10.1109/TSTE.2018.2819201>.
- [18] Kayal P, Chanda CK. Optimal mix of solar and wind distributed generations considering performance improvement of electrical distribution network. *Renew Energy* 2015;75:173–86. <https://doi.org/10.1016/j.renene.2014.10.003>.
- [19] Munikoti S, Abujubbeh M, Jhala K, Natarajan B. A novel framework for hosting capacity analysis with spatio-temporal probabilistic voltage sensitivity analysis. *Int J Electr Power Energy Syst* 2022;134:107426.
- [20] Xiao J, Li Y, Qiao X, Tan Y, Cao Y, Jiang L. Enhancing hosting capacity of uncertain and correlated wind power in distribution network with ANM strategies. *IEEE Access* 2020;8:189115–28. <https://doi.org/10.1109/ACCESS.2020.3030705>.
- [21] Liuayacc-Blas R, Kepplinger P. Violation-mitigation-based method for PV hosting capacity quantification in low voltage grids. *Int J Electr Power Energy Syst* 2022; 142:108318.
- [22] Ochoa LF, Dent CJ, Harrison GP. Distribution network capacity assessment: Variable DG and active networks. *IEEE Trans Power Syst* 2010;25:87–95. <https://doi.org/10.1109/TPWRS.2009.2031223>.
- [23] Alturki M, Khodaei A, Paaso A, Bahramirad S. Optimization-based distribution grid hosting capacity calculations. *Appl Energy* 2018;219:350–60. <https://doi.org/10.1016/j.apenergy.2017.10.127>.

- [24] Allan RN, Grigg CH, Al-Shakarchi MRG. Numerical techniques in probabilistic load flow problems. *Int J Numer Methods Eng* 1976;10:853–60. <https://doi.org/10.1002/nme.1620100412>.
- [25] Solat S, Aminifar F, Shayanfar H. Distributed generation hosting capacity in electric distribution network in the presence of correlated uncertainties. *IET Gener Transm Distrib* 2021;15(5):836–48.
- [26] Karaki SH, Chedid RB, Ramadan R. Probabilistic performance assessment of autonomous solar-wind energy conversion systems. *IEEE Trans Energy Convers* 1999;14:766–72. <https://doi.org/10.1109/60.790949>.
- [27] Teng JH, Luan SW, Lee DJ, Huang YQ. Optimal charging/discharging scheduling of battery storage systems for distribution systems interconnected with sizeable PV generation systems. *IEEE Trans Power Syst* 2013;28:1425–33. <https://doi.org/10.1109/TPWRS.2012.2230276>.
- [28] Hung DQ, Mithulananthan N, Bansal RC. Integration of PV and BES units in commercial distribution systems considering energy loss and voltage stability. *Appl Energy* 2014;113:1162–70. <https://doi.org/10.1016/j.apenergy.2013.08.069>.
- [29] Quan H, Khosravi A, Yang D, Srinivasan D. A survey of computational intelligence techniques for wind power uncertainty quantification in smart grids. *IEEE Trans Neural Networks Learn Syst* 2019;31(11):4582–99.
- [30] Olauson J, Ayob MN, Bergkvist M, Carpman N, Castellucci V, Goude A, et al. Net load variability in Nordic countries with a highly or fully renewable power system. *Nat Energy* 2016;1:16175. <https://doi.org/10.1038/nenergy.2016.175>.
- [31] Patel S, Ahmed M, Kamalasan S. A novel energy storage-based net-load smoothing and shifting architecture for high amount of photovoltaics integrated power distribution system. *IEEE Trans Ind Appl* 2020;56:3090–9. <https://doi.org/10.1109/TIA.2020.2970380>.
- [32] Majzoobi A, Khodaei A. Application of microgrids in supporting distribution grid flexibility. *IEEE Trans Power Syst* 2017;32:3660–9. <https://doi.org/10.1109/TPWRS.2016.2635024>.
- [33] U.S. Department of Energy Office of Scientific and Technical Information. Technical Report: A survey on wind power ramp forecasting, <https://www.osti.gov/biblio/1008309>; 2011 [Online].
- [34] Wazir A, Arbab N. Analysis and optimization of IEEE 33 bus radial distributed system using optimization algorithm.
- [35] Joshi K, Gokaraju RR. An iterative approach to improve PV hosting capacity for a remote community. In: *IEEE Power Energy Soc Gen Meet (PESGM)*. 2018;2018.
- [36] Southern California Edison. 2020 Static Load Profiles, <https://www.sce.com/regulatory/load-profiles/2020-static-load-profiles>; 2021 [Online].
- [37] National Renewable Energy Laboratory. NSRDB data viewer, <https://maps.nrel.gov/nsrdb-viewer/>; 2021 [Online].
- [38] “Electric Power Systems and Equipment - Voltage Ratings (60 Hz),” ANSI C84.1-2016.
- [39] Energy Information Administration, “wind explained-where wind power is harnessed.”, <https://www.eia.gov/energyexplained/wind/where-wind-power-is-harnessed.php>, March 30, 2022.
- [40] Zhang T, Baldick R, Deetjen T. Optimized generation capacity expansion using a further improved screening curve method. *Electr Pow Syst Res* 2015;124:47–54.
- [41] Grubb MJ. Value of variable sources on power systems. In: *Generation, transmission and distribution*, IEE Proceedings C, vol. 138; 1991. p. 149e65.
- [42] Ueckerdt F, Hirth L, Luderer G, Edenhofer O. System LCOE: what are the costs of variable renewables? *Energy* 2013;61:75. <https://doi.org/10.1016/j.energy.2013.10.072>.
- [43] Holttinen H, OMalley M, Dillon J, Flynn D, Keane A, Abildgaard H, et al. Steps for a complete wind integration study. Presented at the 46th Hawaii International Conference on System Sciences Proceedings 2013. p. 2261e70.

Further reading

- [10] Chihota MJ, Bekker B, Gaunt T. A stochastic analytic-probabilistic approach to distributed generation hosting capacity evaluation of active feeders, *International Journal of Electrical Power & Energy Systems* 2022;136:107598.